Scientia Iranica B (2016) 23(1), 277–284

Sharif University of Technology
Scientia Iranica
Transactions B: Mechanical Engineering
www.scientiairanica.com

An Eulerian-Lagrangian model to study the operating mechanism of Stirling pulse tube refrigerators

A. Kardgar, A. Jafarian* and M. Arablu

Faculty of Mechanical Engineering, Tarbiat Modares University, Tehran, P.O. Box 14115-143, Iran.

Received 6 September 2014; received in revised form 13 November 2014; accepted 16 February 2015

KEYWORDS
Eulerian-Lagrangian model;
Pulse tube refrigerator;
Numerical simulation;
Enthalpy flow.

Abstract. This paper aims to study the operating mechanism of Stirling Pulse Tube Refrigerators (PTRs) by tracing the characteristics of working gas elements at the cold end of the system using both Eulerian and Eulerian-Lagrangian (E-L) methods. The main objective of the investigation is to demonstrate non-symmetry effects in the pulse tube section of the system. Elemental cyclic-enthalpy transfer of Simple (S), Double-Inlet (DI) and Multi-Mesh regenerator (MM) PTRs are also investigated to demonstrate the effects of DI and MM systems on the refrigeration mechanism of PTRs. It is shown that the elemental cyclic-enthalpy transfer of SPTR is less than that of DIPTR, MMPTR and MMDIPTR. Also, its elemental cyclic-temperature reduction is more than the others, because the mass flow rate upon the cold end of the SPTR is less than the others. Regarding the reduction of losses in DIPTR and MMPTR, their cold end mean pressure and density increase, and this, consequently, leads the cold end mass flow rate and cyclic-enthalpy transfer to increase. Increase in the enthalpy transfer of MM-PTR, MM-DIPTR and DIPTR consequently improves their cooling performance.

1. Introduction

The operating mechanism of PTRs has been of great interest and one of the most challenging topics of the cryogenics community since its invention by Gifford and Longsworth in 1963 [1]. Due to the complexity of interwoven heat transfer and oscillating fluid flow phenomena in different porous and non-porous sections of the PTRs, many efforts have been dedicated towards developing a sufficiently accurate model for illustrating the operating mechanism of the system. However, few models have been even partially successful in demonstrating this complex mechanism.

Some models treat the entire system, while others concentrate on specific parts of the system, such as the pulse tube or regenerator sections. All numerical models are generally divided into two basic categories:

1. Thermodynamics models;
2. Fluid dynamics models [2].

Thermodynamics models are very important for understanding the physical processes occurring in different parts of the PTR. However, they are time-averaged and only offer a qualitative prediction of PTR performance [3-5]. Thus, for a more accurate prediction of pulse tube performance, compressible oscillating gas flow must be analyzed using full time-dependent models of fluid dynamics. The fluid dynamics models are generally divided into two basic categories:

1. Harmonic analysis;
2. Computational Fluid Dynamics (CFD) models [2].

Since harmonic analysis is capable of performing rapid optimizations, in respect to the dimensions and operational conditions of the PTR, it is widely used as a

*. *Corresponding author. Tel.: +98 21 82884918; E-mail addresses: amin.kardgar@modares.ac.ir (A. Kardgar); jafarian@modares.ac.ir (A. Jafarian); m.arablou@modares.ac.ir (M. Arablu)*

PTR development tool. Nevertheless, this approach is restricted to small-amplitude harmonic pressure variations in the system.

There are two basic approaches in CFD:

1. Eulerian method;
2. Lagrangian method.

Eulerian methods, predominant CFD models of the PTRs [6-8], provide a holistic viewpoint that is very successful in calculation of the characteristics of the PTRs, such as COP and temperature or pressure distributions along the system. On the contrary, Lagrangian methods that follow the characteristics of particles or elements of fluids are very successful in the demonstration of physical processes occurring in the system [9-11]. For instance, by following the elements of fluids that oscillate upon the cold end of the pulse tube section, the cooling mechanism in the system is clarified. This method is known as the characteristics model in the cryogenics community.

Thanks to five decades of research into different aspects of PTRs, it is now theoretically clear that the heat transportation mechanism through the pulse tube section of the system (from cold heat exchanger to hot heat exchanger) occurs due to two different well-known phenomena; surface heat pumping and enthalpy transfer (non-symmetry) effects [12,13]. Although surface heat pumping is the main mechanism of heat transfer in basic PTR, and has no buffer and Orifice/Inertance Tube (O/IT), O/ITPTRs do not rely on surface heat pumping, but on enthalpy transfer into the pulse tube from the regenerator and out of the pulse tube through the O/IT at the hot end of the pulse tube. Both surface heat pumping and non-symmetry effect are the mechanisms of heat transfer in the pulse tube of SPTRs. However, the operating conditions of DIPTRs or even closed multistage PTRs that bring about complex phenomena, such as DC flow effects, are somewhat different from the SPTRs [14].

Laing and Rolland illustrated the operating physics of OPTRs using a thermodynamic non-symmetry effect [10]. This effect is due to phase difference between mass flow rate and pressure through the regenerator and the pulse tube of the system. Arablu and Jafarian [8] improved the performance of PTR by synchronous utilization of a double inlet and multi-mesh regenerator. The mechanism of this improvement relies on modification of the non-symmetry effect in the pulse tube, and also the increase of pressure oscillation amplitude through it due to the decrease of losses by the multi-mesh regenerator and the double inlet.

Following the literature, it is shown that all the characteristics models which have tackled the cooling mechanism of PTRs use some unrealistic assumptions, which lead to a lack of fluency in their aim of demonstrating all the phenomena in the PTRs [9,10]. This work aims to investigate how surface heat pumping and the non-symmetry effect lead to net cyclic enthalpy flow through the pulse tube against a temperature gradient using the Eulerian and the E-L CFD models. To this end, using the characteristics model, a pre-developed 1-D Eulerian CFD code [8] is further developed to trace the elements of fluid oscillating upon the cold end of the pulse tube during a cycle of piston motion under quasi-steady conditions. Since the Eulerian model provides the necessary information for E-L simulations, the E-L model uses real pressure, temperature and mass flow oscillation profiles, and the phase difference between them, in the characteristics model; this is the main reason for opting for Eulerian and E-L models.

2. Physical model and governing equation

To track the gas elements entering and exiting the pulse tube, the domain of PTR is firstly solved by the Eulerian method and then the elements are tracked using the characteristics of the solved domain as the boundary condition for the Lagrangian method.

2.1. Eulerian approach

The schematic of a DIITPTR is shown in Figure 1. For the Eulerian method, the domain is divided into finite volumes. Finite volumes and their centers are shown in Figure 1. All the solution procedures in the Eulerian method are the same as those used in [8].

The continuity, momentum, energy of gas, energy of solid and state equations can be, respectively, represented as follows:

$$\partial(m)_{cv,i}/\partial t = [\dot{m}]_{f,i+1}^{f,i}, \tag{1}$$

$$\partial(mu)_{f,i}/\partial t = [\dot{m}u]_{cv,i}^{cv,i-1} + A_i[P]_{cv,i}^{cv,i-1} - \left[\varepsilon\mu/(K\rho) + c_F\varepsilon^2|u|/K^{\frac{1}{2}}\right]_{f,i}\dot{m}_i\delta x_i + m_{f,i}g\cos\theta, \tag{2}$$

$$\frac{\partial}{\partial t}\left(m\frac{u^2}{2} + mC_vT\right)_{cv,i} = \left[\dot{m}\frac{u^2}{2} + \dot{m}C_pT - kA\frac{\partial T}{\partial x}\right]_{f,i+1}^{f,i} + \alpha_iA_{L,i}\left(T_{s,i}^j - T_i^j\right) - P_i\frac{dV_i}{dt}, \tag{3}$$

$$\frac{\partial}{\partial t}(m_sC_sT_s)_{cv,i} = \left[\lambda_sk_sA_s\frac{\partial T_s}{\partial x}\right]_{f,i+1}^{f,i} + \alpha_iA_{L,i}\left(T_i^j - T_{s,i}^j\right) + \dot{q}_CV_{s,cv,i}, \tag{4}$$

$$P_i^jV_i = m_i^jRT_i^j. \tag{5}$$

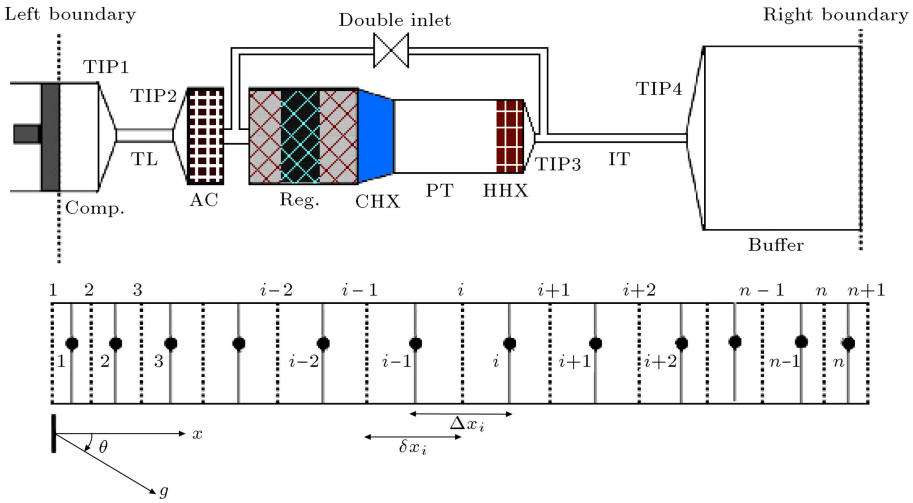

Figure 1. Schematic of a DIPTR and the physical domain [8].

2.2. Lagrangian approach

For tracking the gas particles from a Lagrangian viewpoint, continuity and energy equations are used [9]:

$$\frac{\partial \rho}{\partial t} + \frac{\partial(\rho u)}{\partial x} = 0. \tag{6}$$

The heat conduction is negligible and the gas is ideal. Then, the energy equation can be simplified as follows:

$$\frac{\partial P}{\partial t} + u\frac{\partial P}{\partial x} - a^2\left(\frac{\partial \rho}{\partial t} + u\frac{\partial \rho}{\partial x}\right) = 0. \tag{7}$$

Combining Eqs. (6) and (7), one can write:

$$\frac{\partial P}{\partial t} + u\frac{\partial P}{\partial x} + a^2\rho\frac{\partial u}{\partial x} = 0. \tag{8}$$

For ideal gas:

$$a^2 = kP/\rho. \tag{9}$$

Substituting Eq. (9) into Eq. (8), the following can be written:

$$\frac{\partial P}{\partial t} + u\frac{\partial P}{\partial x} + kP\frac{\partial u}{\partial x} = 0. \tag{10}$$

Neglecting pressure drop in the pulse tube gives:

$$\frac{\partial P}{\partial t} + kP\frac{\partial u}{\partial x} = 0. \tag{11}$$

Rearranging Eq. (11), the velocity in the pulse tube is calculated as follows:

$$u = u_h + \frac{1}{KP}\frac{dP}{dt}(L - x), \tag{12}$$

where, L is the length of the pulse tube, u_h is hot end velocity, and u is gas velocity at the pulse tube. Using a characteristic direction [9]:

$$\left(\frac{dx}{dt}\right)_{\text{char}} = u, \tag{13}$$

and combining Eq. (13) with Eq. (12) leads to:

$$\frac{dx}{dt} = u_h + \frac{1}{KP}\frac{dP}{dt}(L - x). \tag{14}$$

Solving ordinary differential equation (14), one can write:

$$x = L\left[1 - \left(\frac{P_0}{P}\right)^{1/k}\right] + P^{-1/k} \times \int_{t0}^{t} u_h P^{1/k} dt + x_0\left(\frac{P_0}{P}\right)^{1/k}. \tag{15}$$

The gas particle starts entering the pulse tube from $x = x_0 @\ t = t_0$, when the pressure at the pulse tube is $P = P_0$; u_h can be calculated by Eulerian equations.

For calculating temperature variations of gas particles, an isentropic equation is used:

$$T(t) = T_0\left(\frac{P(t)}{P_0}\right)^{(k-1)/k}. \tag{16}$$

A sub-code is developed to solve E-L equations. For calculating the enthalpy, which is carried by each element, Eq. (17) is used:

$$H_{i,\text{out}} - H_{i,\text{in}} = m_i c_{P,i}(T_{i,\text{out}} - T_{i,\text{in}}). \tag{17}$$

3. Results and discussions

3.1. Simple PTR

According to time discretization, the working gas is divided into n elements. To analyze the gas elements, four specific elements, named I, J, K and N, are considered with the respective characteristics shown in Figure 2. Each element enters the pulse tube at a specific time with specific pressure and temperature. Characteristics of the PTR used in this study are

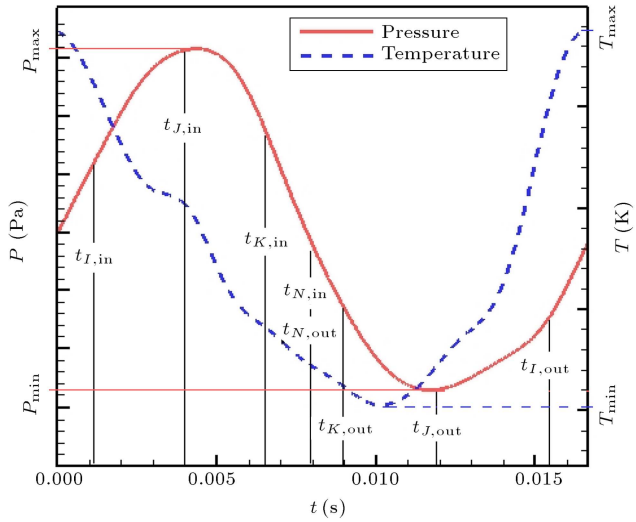

Figure 2. Pressure and temperature at the cold end of the pulse tube section.

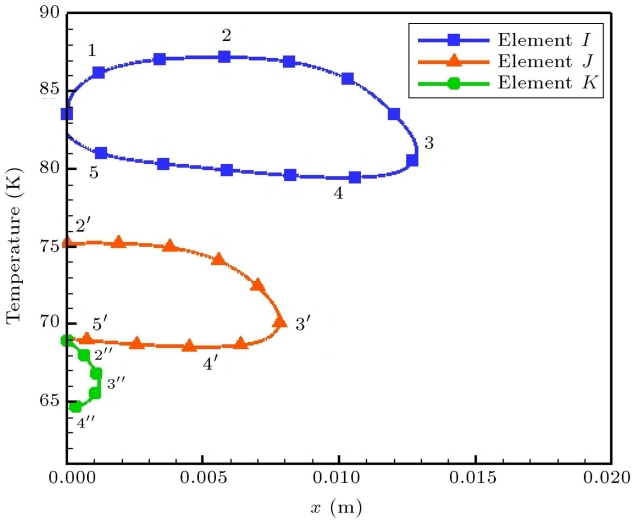

Figure 3. T-x diagram of elements I, J and K.

Table 1. Dimensions of simulated PTR according to Figure 1.

Components	Radius (mm)	Length (mm)
Comp.	21.0088	$7 + 6(x_{amp} + x_d)$
Tip1	-	5
TL	2.5	50
Tip2	-	5
AC	9.25	10
Reg	9.25	45
CHX	-	6
PT	7.7	45
HHX	7.7	7
Tip3	-	5
IT	1.2	1500
Tip4	-	5
Buffer	30	88.42

shown in Table 1. x_{amp} and x_d are the piston motion amplitude and length of the compressor dead volume, respectively. The filling pressure of the system is set to be 2.5 MPa, with an operating frequency of 60 Hz [8].

In the developed code, there is an interchange between the mass flow rate in the Eulerian model and the mass of gas elements in the Lagrangian model. Thus, the mass of gas elements entering the cold end of the pulse tube can be calculated using the mass flow rate in this section, accompanied by the velocity of the hot end as a boundary condition. As shown in Figure 2, the gas element which enters at $t_{I,in}$ is named element I. This element is the last element which exits the pulse tube, too. The element which enters $t_{I,in}$ with maximum pressure is called element J. Element K enters after element J, and element N is the last and first element to enter and exit the tube, respectively. Now, the behavior of these elements is analyzed throughout the pulse tube.

The $T - x$ diagram of elements I, J and K is shown in Figure 3. In process 1-2, the pulse tube pressure is between the buffer's and the maximum pressure, $P_b < P_{pt} \leq P_h$; working gas enters the tube from the cold head and exits from the hot end. Element I enters the pulse tube at pressure P_1, and moves towards the hot end while is compressed isentropically with an increase in its temperature. In process 2-3, the pressure is still between the buffer's pressure and the maximum pressure. In this process, the gas also enters the tube and exits from the hot end. In process 2-3, the piston is in nearly the right position (maximum volume of compressor) and the speed of piston motion is very small, so the mass flow rate in the cold head is also rather small. Furthermore, the pressure approaches its maximum value, so that mass flow at the hot end of the pulse tube (that is, a function of the pulse tube pressure and buffer pressure) tends to a higher value. Consequently, the mass (and density) of gas inside the pulse tube decrease, which causes a pressure reduction. Because of flow work done by the expansion of gas, the temperature of the gas decreases, according to the energy equation. Based on the energy equation, the temperature variation is due to adiabatic compression and expansion of gas. The temperature of the element at point 3 is:

$$T_{I,3} = T_{I,1} \left(\frac{P_{I,3}}{P_{I,1}} \right)^{(k-1)/k}. \quad (18)$$

In process 3-4, the pressure is $P_l < P_{pt} \leq P_b$. The pressure decreases in the pulse tube causes element I to expand and its temperature to decrease. In this process, gas exits the cold head and enters the hot end. In process 4-5, the pressure is $P_l < P_{pt} \leq P_b$. In this process, the pressure increases, causing the gas to be

compressed and its temperature to be increased. The temperature of the gas element at the end of the whole process is less than the temperature at the onset.

$$T_{I,\text{out}} = T_{I,\text{in}} \left(\frac{P_{I,\text{out}}}{P_{I,\text{in}}} \right)^{(k-1)/k} < T_{I,\text{in}}. \quad (19)$$

Element J enters the pulse tube, at $t_{J,\text{in}}$, and follows the process shown as $2'$-$3'$-$4'$-$5'$. As shown in Figure 3, element J enters with $T_{J,\text{in}}$ and exits with a lower temperature, $T_{J,\text{out}}$.

$$T_{J,\text{out}} = T_{I,\text{in}} \left(\frac{P_{J,\text{out}}}{P_{J,\text{in}}} \right)^{(k-1)/k} < T_{J,\text{in}}. \quad (20)$$

Regarding Figure 3, element J enters with maximum pressure and exits with minimum pressure. Thus, it has a maximum temperature reduction, which is simply calculated as follows:

$$\Delta T_{J,\text{out}} = T_{J,\text{in}} - T_{J,\text{out}} = \Delta T_{\max}. \quad (21)$$

Element K enters with $P_{K,\text{in}}$ at $t_{K,\text{in}}$ and exits with a slightly lower pressure. This element follows the process shown as $2''$-$3''$-$4''$. Finally, element N is the last element to enter and the first one to exit the pulse tube, in order that neither its pressure nor its temperature changes. Regarding Figure 2, each element enters with specific pressure and exits with a pressure lower than the entrance pressure. Therefore, each element has a specific cooling capacity. This specific cooling capacity for each element is shown in Figure 4. The elements entering firstly and lastly have the least temperature reduction, while the elements that enter with higher pressure have higher temperature reduction. Consequently, they have a higher cooling capacity.

Integrating all the enthalpy carried by all the elements in a cycle, the enthalpy flow can be calculated.

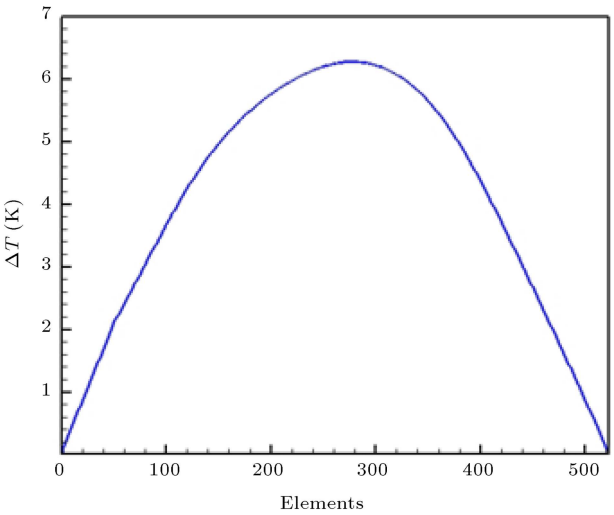

Figure 4. Temperature reduction of each element.

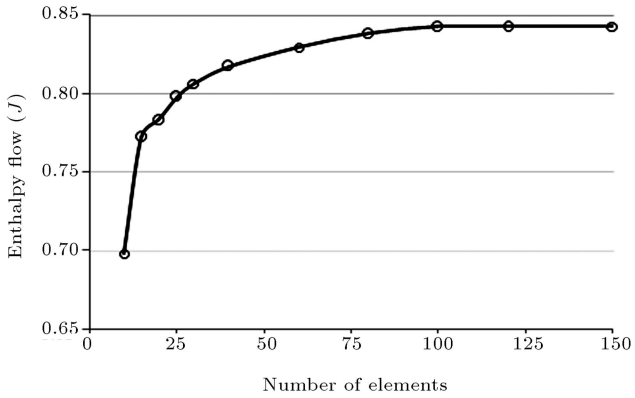

Figure 5. Independency of net enthalpy flow from number of gas elements.

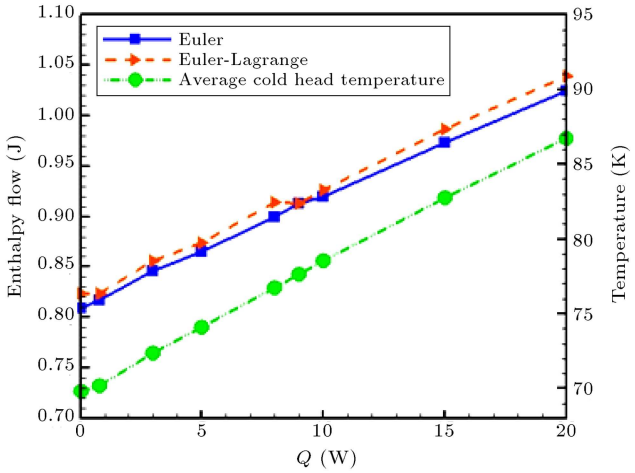

Figure 6. Enthalpy flow carried by all elements and average cold heat exchanger temperature versus cooling power.

Herein, a different number of elements for calculation of the enthalpy flow through the pulse tube are utilized to investigate the element independency, as shown in Figure 5.

As shown in Figure 5, the number of elements at about 100 is the optimum choice. The enthalpy flow of different CHX load conditions is shown in Figure 6. There is a good agreement between the results of the Eulerian and the E-L model results. Since the validity of the Eulerian model results were previously verified by experimental values [8], the accuracy of the E-L model is also validated. Increasing the cooling load of CHX causes the enthalpy flow carried by gas elements to be increased. It can be seen that as the cooling power load increases, the average temperature of the cold head increases. The cooling load amassed by the heat capacity of the elements flows towards the CHX.

3.2. *Effects of double inlet and multi-mesh regenerator on COP*

The COPs of PTRs have almost always been the first concern of researchers. A great deal of research

has been conducted to reduce the losses in these refrigerators. Thanks to this research, it is now crystal clear that approximately 80% of the losses occur in the regenerator [8]. Introducing a double inlet has been the most intelligent method of reducing the regenerator losses, which leads to an increase in amplitude of pressure oscillation through the pulse tube by carrying a small portion of regenerator flow (about 10 percent of total flow) through a bypass [13,14]. According to our previous investigations, the optimum ratio of the double inlet mass flow to the regenerator mass flow in the PTR studied in this work is about 0.138 [8]. Furthermore, using a multi-mesh regenerator, with the aim of decreasing its hot end losses, is another useful method that can cause a substantial improvement in the performance of the system, especially in synchronous applications with a double inlet.

Hereinafter, the mechanism of double inlet and multi-mesh regenerator effects on the improvement of the cooling capacity of the system is quantitatively studied by the E-L model. In this respect, maximum mass flow rate and ratio of maximum to minimum pressure at the cold end of the pulse tube section of different PTRs resulted from Eulerian simulations are firstly considered, as shown in Table 2. Then, elemental enthalpy flow, net cyclic enthalpy flow, cold head temperature and the difference in element inlet and outlet temperatures for different PTRs resulted from the E-L model are investigated, as shown in Figures 7 to 10, respectively.

As shown in Table 2, the ratio of maximum to minimum pressure increases when a double inlet or multi-mesh regenerator is used instead of a simple PTR. In the case of MMDIPTR, which has the highest maximum to minimum pressure ratio, this ratio is approximately 7.5% more than that of a simple PTR. Furthermore, as shown in Table 2, the increase of pressure ratio leads to a perceptible increase of maximum mass flow rate at the cold end. The increase of mass flow rate at the cold end of the system is anticipated to increase the cooling capacity of the system.

As shown in Figure 7, most gas elements of MMDIPTR carry more enthalpy flow and produce more cooling power than the other PTRs. This causes corresponding higher net cyclic enthalpy flow and lower cold head temperature, as shown in Figures 8 and 9. According to Figure 10, the temperature reduction of gas elements in a simple PTR is more than the others, but its elemental enthalpy transfer

Table 2. Maximum mass flow rate and ratio of maximum to minimum pressure at the cold end of the pulse tube section for different PTRs.

	P_{max}/P_{min}	Maximum (kg/s)
Simple PTR	1.241986	0.0076
Double inlet PTR	1.274654	0.0108
MMPTR	1.300959	0.0121
MMDIPTR	1.335024	0.0139

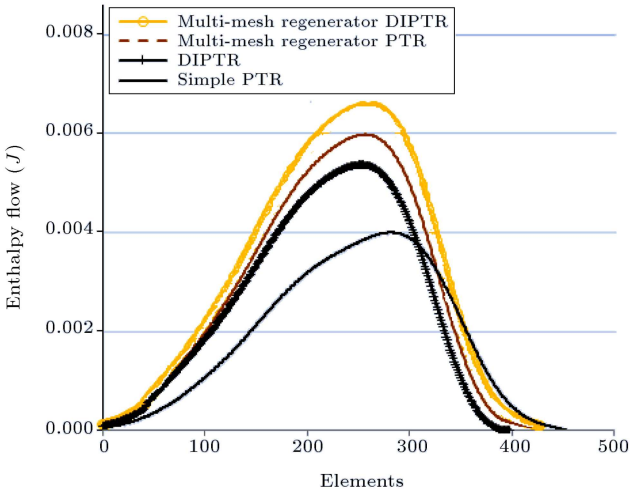

Figure 7. Enthalpy flow carried by gas elements in different PTRs.

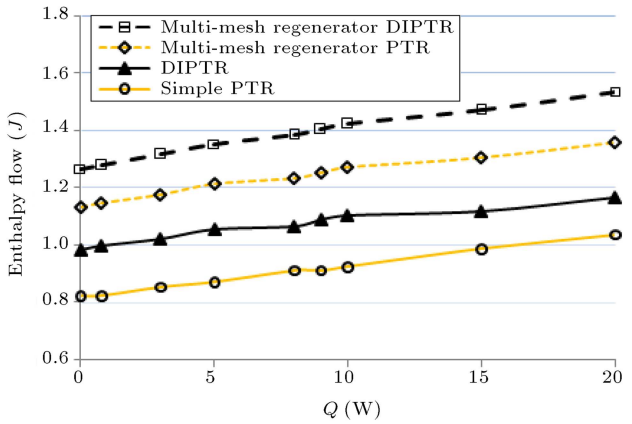

Figure 8. Net enthalpy flow as a function of cooling power for different PTRs.

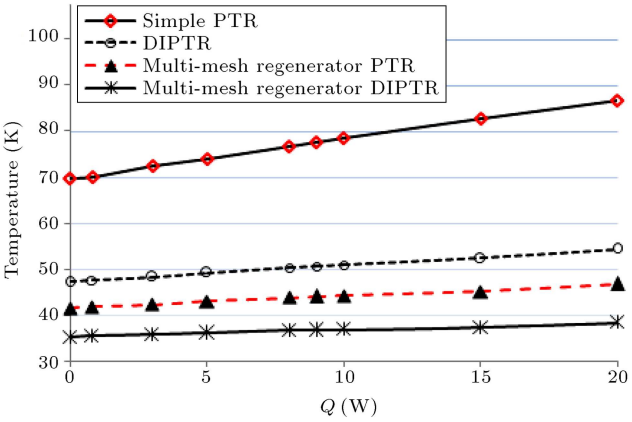

Figure 9. Cyclic-average temperature of cold heat exchanger versus cooling power for different PTRs.

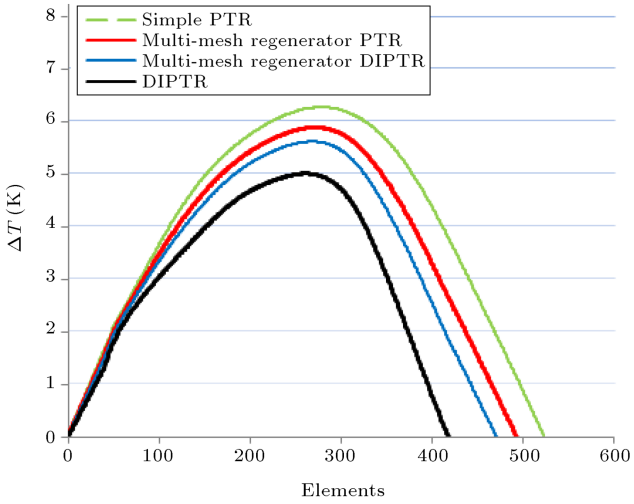

Figure 10. Elemental temperature reduction for various PTRs.

is lower than theirs. It is of paramount importance to know that the enthalpy flow is due to elemental temperature reduction and, also, the mass flow of the elements. As aforementioned, the increase of oscillating pressure amplitude at the cold end of the system causes the mass flow oscillation amplitude to increase and, consequently, the enthalpy flow increases. Thus, there is a compromise between mass flow rate and elemental temperature reduction at the cold end of the system, which sets the net cyclic enthalpy flow in this section.

4. Conclusion

The cooling mechanism at the pulse tube section of Stirling PTRs was studied using an Eulerian-Lagrangian approach. After simulation of a PTR by the Eulerian method, the working gas was divided into a few elements and each element was tracked upon the pulse tube cold end using a Lagrangian method. Simulation results show that the pressure reduction of the elements, which enter and exit the cold end of the pulse tube section during a cycle of piston motion, causes their expansion and a decrease in their temperature. The enthalpy transfer of each element was calculated, and the cooling capacity of SPTR, DIPTR, MMPTR, and MMDIPTR were compared. It was shown that the best elemental enthalpy flow and, consequently, the highest net cyclic enthalpy flow corresponds to MMDIPTR; MMPTR and DIPTR were posed in the second and third level. Elemental temperature reduction in SPTR was higher than the others, although its elemental enthalpy transfer was lower. It was shown that this superficial paradox is due to the effect of mass flow rate on the enthalpy flow. Since mass flow rate in the cold end of the simple PTR is lower than the others, its enthalpy flow is lower than theirs.

Nomenclature

a	Sound velocity
A_L	Interfacial heat transfer area
AC	After Cooler
char	Characteristic
C_p	Specific heat at constant pressure
C_v	Specific heat at constant volume
C_F	Forchheimer's initial coefficient
CHX	Cold Heat Exchanger
COP	Coefficient Of Performance
DI	Double Inlet
g	Gravity acceleration
HHX	Hot Heat Exchanger
IT	Inertance Tube
k	Heat capacity ratio
K	Permeability
L	Tube length
$\dot{m}$	Mass flow rate
MM	Multi-Mesh
P	Pressure
PTR	Pulse Tube Refrigerator
$\dot{q}_c$	Cooling power/CHX solid matrix volume
R	Gas constant
Reg	Regenerator
t	Time
T	Temperature
V	Volume
TL	Transition Line
u	Axial velocity
x	Axial coordinate
θ	System angle with respect to gravity
α	Heat transfer coefficient
ρ	Density
ε	Porosity

Subscripts

b	Buffer
H	Hot end
pt	Pulse tube
max	Maximum
min	Minimum

References

1. Gifford, W.E. and Longsworth, R.C. "Pulse tube refrigeration progress", *Advances in Cryogenic Engineering*, **10B**, pp. 69-77 (1965).

2. Lyulina, I. "Numerical simulation of pulse-tube refrigerators", PhD Thesis, Eindhoven University of Technology (2004).
3. Steijaert, P.P. "Thermodynamical aspects of pulse-tube refrigerator", PhD Thesis, Eindhoven University of Technology (1999).
4. De Waele, A.T.A.M., Steijaert, P.P. and Gijzen, J. "Thermodynamical aspects of pulse tubes I", *Cryogenics*, **37**, pp. 313-324 (1997).
5. De Waele, A.T.A.M., Steijaert, P.P. and Gijzen, J. "Thermodynamical aspects of pulse tubes II", *Cryogenics*, **38**, pp. 329-335 (1998).
6. Boroujerdi, A.A., Ashrafizadeh, A. and Mousavi Naeenian, S.M. "Numerical analysis of Stirling type pulse tube cryocoolers", *Cryogenics*, **51**, pp. 521-529 (2011).
7. Zhu, S. and Matsubara, Y. "Numerical method of inertance tube pulse tube refrigerator", *Cryogenics*, **44**, pp. 649-660 (2004).
8. Arablu, M. and Jafarian, A. "Investigation of synchronous effects of multi-mesh regenerator and double-inlet on performance of a Stirling pulse tube cryocooler", *Cryogenics*, **54**, pp. 1-9 (2012).
9. Xu, M.Y., He, Y.L. and Chen, Z.Q. "Analysis of an orifice pulse tube refrigerator using the method of characteristics", *Cryogenics*, **39**, pp. 751-757 (1999).
10. Liang, J., Ravex, A. and Rolland, P. "Study on pulse tube refrigeration. Part 1: Thermodynamic nonsymmetry effect", *Cryogenics*, **36**, pp. 87-93 (1996).
11. De Boer, P.C.T. "Characteristics of the double inlet pulse tube", *Cryogenics*, **43**, pp. 379-391 (2003).
12. Richardson, R.N. "Pulse tube cryocooler - an alternative cryocooler?", *Cryogenics*, **26**, pp. 331-340 (1986).
13. Radebaugh, R. "Development of the pulse tube refrigerator as an efficient and reliable cryocooler", *Proc. Institute of Refrigeration*, **96**, pp. 11-31 (2011).
14. Zhu, S., Wu, P. and Chen, Z. "Double inlet pulse tube refrigerator: An important improvement", *Cryogenics*, **30**, pp. 514-520 (1990).

Biographies

Amin Kardgar received his BS degree from the University of Tehran, Iran, and his MS degree from Tarbiat Modares University, Tehran, Iran, in Mechanical Engineering (Energy Conversion), in 2010 and 2012, respectively. He is currently a PhD degree candidate at Tarbiat Modares University, Tehran, Iran. His research interests include: mathematical and numerical modeling, computational fluid dynamics, heat transfer in porous media, and turbulent combustion.

Ali Jafarian received BS, MS and PhD degrees from Sharif University of Technology, Tehran, Iran, in 2000, 2002 and 2008, respectively, all in Mechanical Engineering (Energy Conversion). He is currently Professor of Mechanical Engineering at Tarbiat Modares University, Tehran, Iran.

Masoud Arablu received his BS degree from the University of Zanjan, Iran, and his MS degree from Tarbiat Modares University, Tehran, Iran, in Mechanical Engineering (Energy Conversion), in 2010 and 2013, respectively. His research interests include: computational fluid dynamics, heat transfer, pulsating flow, cryogenics, and turbulent combustion.